Analytical Methods

Accepted Manuscript

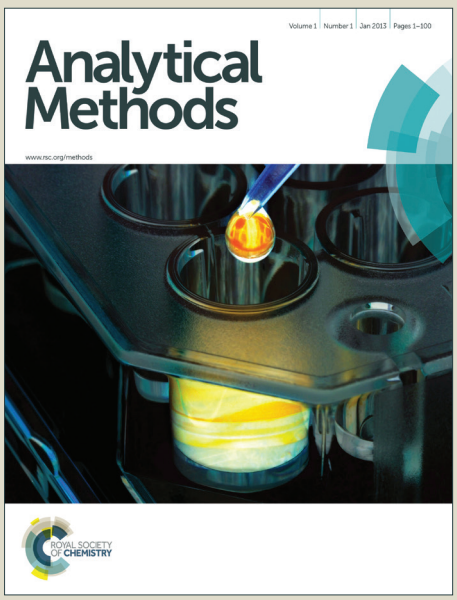

This is an *Accepted Manuscript*, which has been through the Royal Society of Chemistry peer review process and has been accepted for publication.

Accepted Manuscripts are published online shortly after acceptance, before technical editing, formatting and proof reading. Using this free service, authors can make their results available to the community, in citable form, before we publish the edited article. We will replace this *Accepted Manuscript* with the edited and formatted *Advance Article* as soon as it is available.

You can find more information about *Accepted Manuscripts* in the Information for Authors.

ROYAL SOCIETY OF CHEMISTRY

www.rsc.org/methods

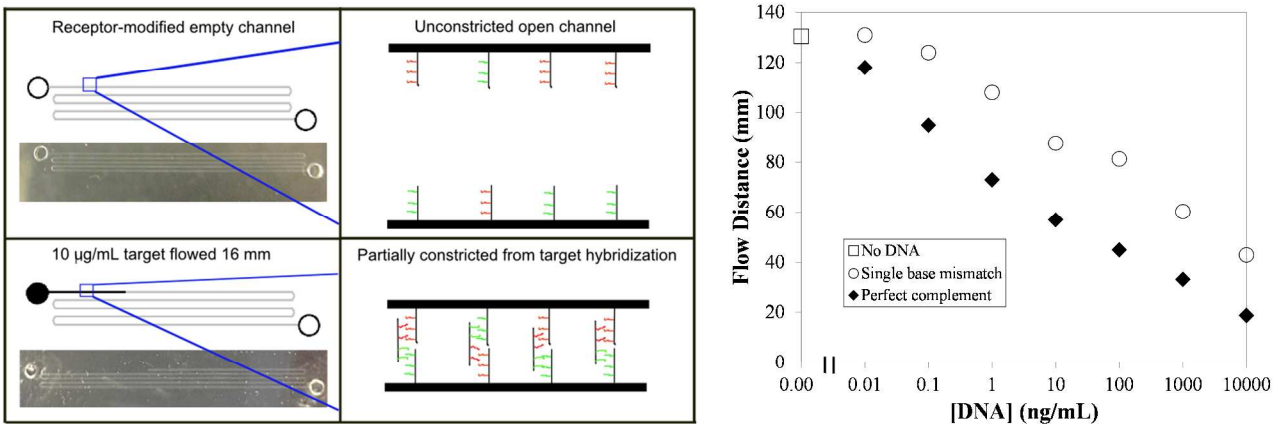

Non-instrumented and label-free point-of-care diagnostic microfluidic devices for quantifying nucleic acids by flow distance measurement.

MICROFLUIDIC DEVICES FOR LABEL-FREE AND NON-INSTRUMENTED QUANTITATION OF UNAMPLIFIED NUCLEIC ACIDS BY FLOW DISTANCE MEASUREMENT

Debolina Chatterjee, Danielle S. Mansfield, and Adam T. Woolley*

Department of Chemistry and Biochemistry, Brigham Young University, Provo, Utah, USA

*Corresponding author: atw@byu.edu

Abstract

Timely biomarker quantitation has potential to improve human health but current methods have disadvantages either in terms of cost and complexity for benchtop instruments, or reduced performance in quantitation and/or multiplexing for point-of-care systems. We previously developed microfluidic devices wherein visually observed flow distances correlated with a model analyte's concentration.[1] Here, we significantly expand over this prior result to demonstrate the measurement of unamplified DNA analogues of microRNAs (miRNAs), biomarkers whose levels can be altered in disease states. We have developed a method for covalently attaching nucleic acid receptors on poly(dimethylsiloxane) microchannel surfaces by silane and cross-linker treatments. We found a flow distance dependence on target concentrations from 10 μg/mL to 10 pg/mL for DNA in both buffer and synthetic urine. Moreover, flow time in addition to flow distance is correlated with target concentration. We also observed longer flow distances for single-base mismatches compared to the target sequence at the same concentration, indicating that our approach can be used to detect point mutations. Finally, experiments with DNA analogues of miRNA biomarkers for kidney disease (mir-200c-3p) and prostate cancer (mir-107) in synthetic urine showed the ability to detect these analytes

near clinically relevant levels. Our results demonstrate that these novel microfluidic assays offer a simple route to sensitive, amplification-free nucleic acid quantitation, with strong potential for point-of-care application.

Introduction

Biomarkers are disease indicators which can be found in body fluids such as blood, saliva or urine and can indicate the disease state and/or progression characteristics.[2-3] The measurement of biomarkers is playing a growing role in early detection of disease, enabling improved treatment. Various biomarkers, including proteins, carbohydrates, lipids, hormones, metabolites and nucleic acids have been correlated with physiological responses to disease, injury, stress, etc.[4]

One class of analysis systems for biomarkers includes high performance benchtop instruments such as mass spectrometers (MS),[5-6] liquid chromatography coupled to MS,[7-8] capillary electrophoresis coupled to MS,[8] Raman spectroscopy,[9] and nuclear magnetic resonance spectroscopy.[10] On the other hand, simplified systems include paper-based microfluidics,[11-14] blood glucose monitors,[15] lateral flow immunoassays,[16] and other point-of-care systems.[17] Many benchtop instruments have desirable performance characteristics such as good detection limits, accuracy, specificity, quantitation and/or multiplexing but the instrumentation is usually expensive and non-portable. In contrast, point-of-care systems are generally inexpensive and quick but lack several desirable performance characteristics such as good detection limits, quantitation capabilities (except for glucose monitoring[15]), and multiplexing.

One important class of nucleic acid biomarkers is microRNA (miRNA), 19-24 nucleotide long, noncoding RNA that blocks translation of messenger RNA and hence plays a critical role in cell

function.[18-19] MiRNAs were first described in 1993 by Lee and collegues.[20] MiRNAs are resistant to RNase activity, and are stable under both temperature and pH extremes,[18] such that conditions for miRNA analysis are somewhat less stringent than for other types of RNA. Furthermore, differential expression of miRNAs in many disease states combined with their presence in serum, plasma and other body fluids, makes them promising biomarkers in early detection, classification, or prognosis of various illnesses including cancer,[21-22] diabetes,[23] kidney disease,[24-25] and liver disease.[26] For example, specific miRNAs are up- or down-regulated in cancer and thus have promise as biomarkers for cancer classification.[18] Mir-141 has elevated levels in the blood of prostate cancer patients, while mir-25 and mir-223 have increased serum levels in lung cancer patients compared to controls.[18] Moreover, differential expression of mir-126 and mir-182 in urine identified bladder cancer,[27] while mir-125a and mir-200a were detected at reduced levels in the saliva of oral squamous cell carcinoma patients compared to healthy controls.[28] Furthermore, mir-29a, mir-181a and mir-652 are potential breast cancer biomarkers,[29] while mir-21, mir-146a and mir-148a show promise to predict lymph node metastasis in gastric cancer.[30]

Accurate measurement of miRNA levels is important but the intrinsic characteristics of miRNAs such as low levels (fg/mL-pg/mL), small size, sequence similarity, and difficulty in selective amplification make detection challenging.[31] Despite the difficulty, some methods have been developed for miRNA measurement. Quantitative reverse transcription PCR (qRT-PCR), which is the gold standard for sequence-specific RNA quantitation, does not work for miRNAs since they are about the same length as standard PCR primers.[32] However, modifications of qRT-PCR using stem loop primers combined with TaqMan probes,[31] enable miRNA measurement with good dynamic range, 1000-fold better sensitivity than hybridization methods and reasonable

target specificity.[31] Yet, this method needs probes, stem-loop primers and a reverse transcription step, all of which increase complexity and assay time. An amplification-based enzymatic bioluminescence miRNA assay[33] provides 10 pg/mL detection limits but the use of enzymes and their costs are downsides. In-situ hybridization with locked nucleic acid probes[34] can determine native locations of miRNAs inside cells and tissues, but requires a fluorescence microscope, and suffers from low throughput and high background signal. Microarray hybridization-based methods[35] for miRNA profiling offer high throughput but require a labeling step for detection thus increasing complexity and cost. Liu et al.[36] recently detected miRNAs through graphene fluorescence and switch-based cooperative amplification, resulting in a 11 fM (~4 fg/mL) limit of detection; however, this method introduces complexity through amplification and labeling. Label-free miRNA detection methods involving nanopores[37] and surface plasmon resonance[38] have also been developed, with detection limits in the mid-fM range. Although sample preparation is simplified because labeling is not needed, sophisticated instruments and/or complex data interpretation are required, thus hindering their use in simple, point-of-care diagnostic settings. Importantly, present methods for miRNA analysis are in need of improvement; thus, as a step toward this we have focused on quantifying DNA analogues of miRNA.

We have developed a novel, label-free, sequence-specific nucleic acid quantitation method wherein the concentration is correlated with capillary flow distance of target solution in receptor-coated microfluidic channels. Devices are made in an elastomer, poly(dimethylsiloxane) (PDMS), that has microfluidic channels covalently derivatized with oligonucleotide receptors that are complementary to the target. Specific hybridization of target to receptors allows constriction through cross-linking of the top and bottom channel surfaces, as illustrated

schematically in Figure S1 in the Electronic Supplementary Information (ESI). This concentration-dependent constriction relates target concentration with the capillary flow distance. Thus, target concentration can be determined readily from the capillary flow distance, which is easily measured through visual inspection. Our detection approach is much simpler than that of Tavares et al.[39] wherein distance measurement was also carried out, but required nucleic acid labeling and fluorescence instrumentation. We have studied DNA analogues of miRNAs and found a flow distance dependence on target concentrations from 10 μg/mL to 10 pg/mL in both buffer and synthetic urine. Furthermore, flow time in addition to flow distance is correlated with target concentration. Our approach offers the ability to detect very low target concentrations (10 pg/mL) and can discern single-base mismatches. Finally, we have analyzed DNA analogues of miRNAs linked to kidney disease and prostate cancer in synthetic urine samples and detected these analytes near clinically relevant levels (~5 pg/mL).[40] Our novel quantitation method's simplicity and cost effectiveness combines performance, selectivity and speed, thus demonstrating excellent potential for wide application in point-of-care nucleic acid biomarker diagnostics.

Experimental Section

Mold preparation and PDMS device fabrication followed nearly the same procedures we published earlier,[1] but using a different positive photoresist, AZ4620 (AZ Electronic Materials, Branchburg, NJ). Although rounded microchannel cross sections were used as before[1] because of the ease of fabrication, alternate channel geometries such as sigmoidal or trapezoidal could be explored if more complex molds could be made readily. The microchannels in the devices used for flow distance experiments were 11 μm tall and 58 μm wide with a 0.5 mm PDMS top layer

thickness. Other channel heights (7-18 μm) were used for initial surface modification optimization. All DNA oligonucleotides were obtained from Operon Biotechnologies (Huntsville, AL); names and sequences are given in Table 1. Single-base mismatches were selected to demonstrate sequence specificity, rather than for clinical relevance.

Procedure for experimentation. The basic protocol for surface modification in the DNA sensing platform is outlined schematically in Figure S2 in the ESI and described below. 3-aminopropyl-diisopropylethoxysilane (APDIES, Gelest, Morrisville, PA, 1-5% v/v in methanol) was filled via a combination of capillary action and/or vacuum in plasma-bonded PDMS microchannels of 7-18 μm heights. The silane was allowed to attach covalently to the PDMS channel walls for 30-60 min, leaving exposed amine groups (see Figure S2B). Then the APDIES solution was removed and the channels were flushed with phosphate buffered saline (PBS, 10 mM, pH 7.2) to remove unattached material. Next, PBS was aspirated from the channels and glutaraldehyde solution (Sigma-Aldrich, St. Louis, MO, 0.5-8% v/v in water) was added to the channels to react with APDIES amine groups, as seen in Figure S2C, for 30-60 min. Then the glutaraldehyde solution was removed and channels were once again flushed with PBS. Some initial experiments with (3-glycidyloxypropyl)trimethoxysilane (GOPS, Sigma-Aldrich, 1-10% v/v in methanol) instead of APDIES were also conducted using the same protocol as above but without glutaraldehyde reaction with the silanized surface. Next, PBS was aspirated from the channels and 2 μL of a 2 mg/mL amine-modified DNA oligonucleotide solution (50/50 mixture of two receptor sequences in 10 mM PBS) was filled in the channels by capillary action followed by 1 hour incubation to react with the free aldehyde in glutaraldehyde. After this, channel emptying followed by rinsing with PBS were done as above. During all the incubation steps, the devices were stored in a humidified ambient to prevent drying. After emptying the channel by applying vacuum, 1 μL of

DNA target solution of specified concentration in PBS or simulated urine (VWR, West Chester, PA) was pipetted into the reservoir. The flow distance of the target solution in the microchannel was measured with a ruler, and photographs of the devices were obtained with a digital camera. Experiments for determining flow distance as a function of time were also performed with buffer (no DNA) or target solutions; flow distance was measured every 10 seconds until the fluid receded back to the sample introduction point. Experiments with mismatched sequences (see Table 1) of specified concentration in PBS were conducted under the same protocol as for the complementary DNA target. Also, experiments were conducted with DNA analogues of miRNA, mir-200c-3p and mir-107, in PBS and simulated urine with their respective amine-modified receptors attached to channel surfaces (see Table 1).

Results and Discussion

We studied nucleic acid sensing in a flow distance microfluidic platform. We measured the flow profiles of target and control (buffer) solutions as a function of time in the derivatized microchannels. In addition, we characterized the maximum flow distances for different concentrations of various DNA oligonucleotides, including a complementary DNA target sequence, single-base and fully mismatched sequences, and DNA analogues of miRNA targets.

Figure S3 in the ESI shows schematics as well as photographs of microchannels before and after the addition of target solutions. Figure S3A shows an unfilled channel that is clearly visible in the photograph, while Figure S3B shows a microchannel partially filled with buffer solution that can be easily distinguished from the unfilled portion. In our prior work, buffer solution flowed to the end of 13-17 μm tall channels;[1] however, in the current studies, the shorter 11 μm height channels in combination with solution evaporation led to only partial channel filling. In either

case the flow distance can readily be determined by visual examination. Figures S3C and S3E show shorter flow distances for 10 μg/mL model target DNA concentrations in buffer and synthetic urine respectively, while Figures S3D and S3F show longer flow distances for 10 ng/mL (lower concentration) model target in these same matrices. These results agree with our expectation that higher target concentrations cause more rapid channel constriction which leads to shorter flow distances, while lower target concentrations result in slower channel constriction that yields longer flow distances, as we showed previously.[1]

In initial experiments we derivatized microchannels with GOPS in an effort to attach amine-modified DNA receptors to plasma-oxidized microchannels. In a 13 μm tall channel functionalized with 1% GOPS and treated with model receptors 1 and 2 (see Table 1), a high concentration (700 μg/mL) of model target solution travelled 130 mm, a much longer flow distance than we observed for similar concentrations and channels in earlier work involving biotin-streptavidin.[1] We hypothesized that perhaps either a higher GOPS concentration or shorter channel height would decrease the flow distance. However, increasing the GOPS concentration to 8% or reducing the channel height to 7 μm still resulted in a 130-140 mm flow distance for 700 μg/mL solutions of model target. Furthermore, different incubation times (30-180 min) for GOPS were tried, but likewise yielded similar flow distances for the same concentration of model target. From these experiments we concluded that GOPS and amine-linked DNA coupling did not work well in our system, possibly because the reactive epoxy ring had been partially deactivated (before exposure to DNA) by ring opening in the presence of water or methanol –OH groups.[41] Another reason for poor results with GOPS could be that it is a tri-alkoxy silane[42] that can form branched or cross-linked structures that result in multiple layers and poorer uniformity in the coating.

Given the difficulties encountered with GOPS, we also tried surface functionalization with APDIES along with a cross-linker (glutaraldehyde) for receptor attachment. APDIES has just one surface-reactive alkoxy functional group, which results in channel coating with a maximum of a monolayer of silane.[42] In 13 μm tall channels modified using 2% APDIES and glutaraldehyde concentrations of 2%, 5% and 8%, the flow distances for 1-10000 ng/mL model target solution are given in Figure S4 in the ESI. We observe two trends in the data: first, for a given concentration of model target, the flow distance decreases with increasing concentration of the glutaraldehyde cross-linker used in derivatization; second, more marked dependence of flow distance on concentration is observed with increasing glutaraldehyde concentrations. We hypothesize that increased numbers of receptor attachments on the channel surface with higher cross-linker concentrations provide more target-receptor interaction, resulting in more rapid channel constriction and shorter flow distances. With 2% glutaraldehyde, there is little flow distance dependence on concentration. With 5% and 8% glutaraldehyde, there is some flow distance dependence on concentration, and the change in flow distance for each 10-fold concentration change is greater for 8% glutaraldehyde. Thus, 8% glutaraldehyde solution was used for surface derivatization because of the greater sensitivity of flow distance to changes in DNA concentration. We note that solutions with glutaraldehyde concentrations over 8% were so viscous that flow through 13 μm tall channels during successive steps was irreproducible, making further increases in glutaraldehyde concentration impractical. Imine bond formation by reaction of an aldehyde with amine-modified DNA, although less robust than the same linkage after cyanoborohydride reduction, provides simple and direct receptor attachment with adequate stability for subsequent surface characterization.[43]

In 13 μm tall microchannels modified with receptors, 1 ng/mL model target solutions in buffer flowed distances close to those of buffer lacking DNA (130-140 mm). We found that microchannel heights of 11 μm allowed us to determine DNA target concentrations even lower than 1 ng/mL, so this channel height was used in subsequent work. Experiments were conducted to determine flow distance as a function of time for solutions (with or without DNA) travelling through receptor-coated, 11 μm tall microchannels. Figure 1 shows the flow distances for buffer (lacking DNA) and model target DNA (1 μg/mL and 1 ng/mL) in buffer, as a function of flow time in microchannels coated with model receptors 1 and 2. The flow distance for buffer, which does not interact with receptors, increases with flow time until reaching a plateau at 123 mm flow in ~180 seconds. In contrast, the model target in solutions interacts with the surface receptors which constricts the channel (Figure S1B and S1D), and slows the flow velocity. Thus, 1 ng/mL target takes ~450 seconds to travel 80 mm where it stops, compared to ~60 seconds for buffer solution to travel the same distance. Also, 1 μg/mL model target takes ~180 seconds to travel 32 mm where it stops, versus 20 seconds for buffer and 90 seconds for 1 ng/mL model target to travel the same distance. In all experiments, after flow stops the fluid position is maintained for another ~3 min, after which the liquid recedes back to the sample introduction point due to evaporation. We note that this 3 min "plateau" in flow gives ample time for distance measurement. Figure 2 shows a plot of this maximum flow distance as a function of flow time for different model target DNA concentrations. Lower model target concentrations have greater maximum flow distances and flow times. Thus, flow time, in addition to flow distance,[1] could be used to determine the concentration of target in a solution flowed in our devices.

Experiments involving several mismatched sequences were done using 11 μm tall microchannels coated with model receptors 1 and 2. Figure 3 shows the flow distance as a function of logarithm

of DNA concentration for the model target and five mismatched sequences. For the model target sequence the flow distance has a linear correlation with the logarithm of target concentration. The lowest detected model target concentration was 10 pg/mL with a mean flow distance of 118 mm, appreciably less than the buffer (no DNA) mean flow distance (128 mm). The total mismatch sequence flows greater distances (nearly the same as buffer, except for the 10 µg/mL solution) than all the other sequences, indicating that the surface-attached model receptors 1 and 2 do not bind appreciably with the total mismatch sequence in solution flowing through the channel. This result demonstrates the specificity of our system in distinguishing between complementary and non-complementary sequences. Because of this significant difference in flow properties, we decided to test the ultimate in sequence specificity: single-base mismatches. Thus, we tested flow with oligonucleotides that differed from the target only at the 6th position from the 5' end or at the 6th position from the 3' end. As seen in Figure 3, many mismatched sequences had 10-20 mm longer average flow distances than the model target, but shorter flow distances than the total mismatch at each concentration. These longer flow distances for mismatched sequences are driven by their lower energy of hybridization compared to that of the complementary sequence. Our results show that the position of the base mismatch is important in generating a distinct flow distance from the complementary sequence. For example, a single-base mismatch at the 2nd base from the 3' end of model receptor 1 resulted in longer flow distances than a similar mismatch at the 2nd base from the 5' end of this same receptor. Although a more comprehensive study of the effects of mismatches on flow distance should provide further information, our results demonstrate that the binding of surface-attached receptors to target is affected by a difference of just one base in the sequence. Thus, our approach can be used to

differentiate between single-base mismatch point mutations which are often the cause of genetic disorders.[44]

Figure 4 shows flow distances in receptor 1 and 2 modified microchannels as a function of logarithm of model target concentration in buffer and synthetic urine. A linear correlation is seen between flow distance and logarithm of target concentration in both buffer and in synthetic urine, which should enable direct quantitation from the easily measured flow distance. Moreover, the linearity is maintained over a 10^6-fold range of concentrations indicating a wide dynamic range. The lowest concentration of target DNA detected is 10 pg/mL, indicating a 100-fold improvement over what we achieved previously for biotin-streptavidin.[1] Importantly, the lowest concentrations measured in our simple system are as much as 1000-fold lower than other simple diagnostics such as paper-based microfluidic systems that can detect in the high nM range.[45]

Given these detection capabilities, we also tested DNA analogues of a kidney disease miRNA biomarker, mir-200c-3p,[40] and a prostate cancer miRNA biomarker, mir-107,[46] in buffer and synthetic urine (Figure 5). As with previous nucleic acid targets, there is a linear correlation between flow distance and logarithm of nucleic acid concentration with both biomarkers. The lowest concentration detected for both biomarkers is 10 pg/mL, which is near actual concentrations of miRNAs in urine (~5 pg/mL).[40] We see a small increase in the standard deviations of slopes and intercepts of these plots compared to the results for the model target (Figure 4), perhaps due to higher GC content in the miRNA analogues (~48% versus 40%). The miRNA analogues are also one base longer than the model target, but this seems less likely to increase scatter in the data. Importantly, we have shown the ability to detect analogues of significant miRNA biomarkers in a similar matrix and at levels near those that are clinically

significant, demonstrating strong potential for application of our system in quantifying miRNA and other nucleic acids in medical applications.

To move from our present work to miRNA detection in biological samples will require additional advances. First, although miRNAs are resistant to RNase digestion, greater care would likely need to be taken in device and solution preparation. Second, miRNAs are present in exosomes in urine, so methods are needed for making the miRNAs available for hybridization. One method to release miRNA to enable hybridization would be to add a surfactant (or organic solvent) to the urine sample, which would emulsify the exosome lipid bilayer. The viscosity of normal (or diabetic) urine is ~1.2 fold greater than that of water, with a range in viscosity of ~20% over 14 samples, while urine with up to 1% albumin has a viscosity 1.3-1.6 times that of water.[47] We previously found that flow distances in our devices were unaffected (within experimental uncertainty) by viscosity unless it was increased by more than a factor of 2 over that of water.[1] Thus, the viscosity of most urine samples is in a range where flow distances in our devices should be independent of viscosity. Given these considerations, it should be possible to measure miRNA directly from biological fluids such as urine thus showing great potential for point-of-care diagnosis.

Conclusions

We have developed a simple, microfabricated flow-based system for sequence-specific nucleic acid quantitation in biological matrices. We have covalently attached oligonucleotide receptors on poly(dimethylsiloxane) microchannel surfaces through combined silane and cross-linker treatments. We found that flow time in addition to flow distance is correlated with target concentration in our devices. This system can detect specific DNA targets in buffer and synthetic

urine at 10 pg/mL levels. In addition, our approach has a dynamic range of 10^6 and single-base mismatch specificity. Finally, DNA analogues of two miRNA biomarkers have been measured near clinically significant levels, showing great promise for future medical application.

We envision several improvements that can be incorporated to our nucleic acid analysis systems. Branched channel designs would allow different miRNAs to be quantified simultaneously from the same sample or for replicate tests to be done on the same biomarker. Branching channels having at least one segment lacking receptors could also be used to account for viscosity variability in specimens such as urine or blood. Designs with a microchannel extending to the edge of the device would allow direct sample loading without pipetting, thus facilitating point-of-care usage. These improvements for nucleic acid analysis in biological samples should further increase the versatility of our system for rapid and simple biomarker measurement.

Our approach could be extended to other target systems; in addition to miRNA, other RNA or DNA biomarkers could be targeted. Furthermore, our methods could be extended to detect small molecules, ions, or metals through aptamers. For example, surface-attached oligonucleotide receptors would bind to free aptamer, while aptamer bound to target would not hybridize, resulting in flow distance differences between the presence or absence of target. The work described herein, thus demonstrates excellent potential for biological target measurement in a point-of-care setting.

Acknowledgement

We thank the National Institutes of Health (R01 EB006124) for supporting this work.

References

1. D. Chatterjee, D. S. Mansfield, N. G. Anderson, S. Subedi and A. T. Woolley, *Anal. Chem.,* 2012, **84**, 7057-7063.
2. G. J. Kelloff and C. C. Sigman, *Nat. Rev. Drug Discov.,* 2012, **11**, 201-214.
3. P. Boffetta, *Carcinogenesis,* 2010, **31**, 121-126.
4. H. J. Issaq, S. D. Fox, K. C. Chan and T. D. Veenstra, *J. Sep. Sci.,* 2011, **34**, 3484-3492.
5. M. Carrera, B. Cañas, D. López-Ferrer, C. Piñeiro, J. Vázquez and J. M. Gallardo, *Anal. Chem.,* 2011, **83**, 5688-5695.
6. J. R. Whiteaker, L. Zhao, L. Anderson and A. G. Paulovich, *Mol. Cell. Proteomics,* 2010, **9**, 184-196.
7. H. G. Gika, G. A. Theodoridis, R. S. Plumb and I. D. Wilson, *J. Pharm. Biomed. Anal.,* 2014, **87**, 12-25.
8. J. V. Alberice, A. F. S. Amaral, E. G. Armitage, J. A. Lorente, F. Algaba, E. Carrilho, M. Marquez, A. Garcia, N. Malats and C. Barbas, *J. Chromatogr. A,* 2013, **1318**, 163-170.
9. S. Ye, Y. Mao, Y. Guo and S. Zhang, *TrAC, Trends Anal. Chem.,* 2014, **55**, 43-54.
10. E. P. Rhee and R. E. Gerszten, *Clin. Chem.,* 2012, **58**, 139-147.
11. D. Sechi, B. Greer, J. Johnson and N. Hashemi, *Anal. Chem.,* 2013, **85**, 10733-10737.
12. X. Li, D. R. Ballerini and W. Shen, *Biomicrofluidics,* 2012, **6**, 011301.
13. W. Dungchai, O. Chailapakul and C. S. Henry, *Analyst,* 2011, **136**, 77-82.
14. H. Liu and R. M. Crooks, *J. Am. Chem. Soc.,* 2011, **133**, 17564-17566.
15. A. Rebel, M. A. Rice and B. G. Fahy, *J. Diabetes Sci. Tech.,* 2012, **6**, 396-411.
16. M. D. Lindsley, N. Mekha, H. C. Baggett, Y. Surinthong, R. Autthateinchai, P. Sawatwong, J. R. Harris, B. J. Park, T. Chiller, S. A. Balajee and N. Poonwan, *Clin. Infect. Dis.,* 2011, **53**, 321-325.
17. W. Weaver, H. Kittur, M. Dhar and D. D. Carlo, *Lab Chip,* 2014, **14**, 1962-1965.
18. K. Zen and C. –Y. Zhang, *Med. Res. Rev.,* 2012, **32**, 326-348.
19. H. Dong, J. Lei, L. Ding, Y. Wen, H. Ju and X. Zhang, *Chem. Rev.,* 2013, **113**, 6207-6233.
20. R. C. Lee, R. L. Feinbaum and V. Ambros, *Cell,* 1993, **75**, 843-854.
21. W. C. S. Cho, *Biochim. Biophys. Acta,* 2010, **1805**, 209-217.
22. K. Ruan, X. Fang and G. Ouyang, *Cancer Lett.,* 2009, **285**, 116-126.
23. D. S. Karolina, A. Armugam, S. Sepramaniam and K. Jeyaseelan, *Expert Rev. Endocrinol. Metab.,* 2012, **7**, 281-300.
24. J. Ho and J. A. Kreidberg, *J. Am. Soc. Nephrol.,* 2012, **23**, 400-404.
25. M. Liang, Y. Liu, D. Mladinov, A. W. Cowley Jr, H. Trivedi, Y. Fang, X. Xu, X. Ding and Z. Tian, *Am. J. Physiol. Renal Physiol.,* 2009, **297**, F553-F558.
26. X. –M. Chen, *World J. Gastroenterol.,* 2009, **15**, 1665-1672.
27. M. Hanke, K. Hoefig, H. Merz, A. C. Feller, I. Kausch, D. Jocham, J. M. Warnecke and G. Sczakiel, *Urol. Oncol.,* 2010, **28**, 655-661.
28. N. J. Park, H. Zhou, D. Elashoff, B. S. Henson, D. A. Kastratovic, E. Abemayor and D. T. Wong, *Clin. Cancer Res.,* 2009, **15**, 5473-5477.
29. A. M. McDermott, N. Miller, D. Wall, L. M. Martyn, G. Ball, K. J. Sweeney and M. J. Kerin, *PLoS ONE,* 2014, **9**, e87032.
30. S. Y. Kim, T. Y. Jeon, C. I. Choi, D. H. Kim, D. H. Kim, G. H. Kim, D. Y. Ryu, B. E. Lee and H. H. Kim, *J. Mol. Diag.,* 2013, **15**, 661-669.
31. M. Planell-Saguer and M. C. Rodicio, *Clin. Biochem.,* 2013, **46**, 869-878.

32. T. D. Schmittgen, E. J. Lee, J. Jiang, A. Sarkar, L. Yang, T. S. Elton and C. Chen, *Methods,* 2008, **44**, 31-38.
33. Y. Sun, K. J. Gregory, N. G. Chen and V. Golovlev, *Anal. Biochem.,*2012, **429**, 11-17.
34. S. Herzer, A. Silahtaroglu and B. Meister, *J. Neuroendocrin.,* 2012, **24**, 1492-1504.
35. W. Li and K. Ruan, *Anal. Bioanal. Chem.,* 2009, **394**, 1117-1124.
36. H. Liu, L. Li, Q. Wang, L. Duan and B. Tang, *Anal. Chem.,* 2014, **86**, 5487-5493.
37. Y. Wang, D. Zheng, Q. Tan, M. X. Wang and L. Q. Gu, *Nat. Nanotechnol.,* 2011, **6**, 668-674.
38. S. Fang, H. J. Lee, A. W. Wark and R. M. Corn, *J. Am. Chem. Soc.,* 2006, **128**, 14044-14046.
39. A. J. Tavares, M. O. Noor, C. H. Vannoy, W. R. Algar and U. J. Krull, *Anal. Chem.*, 2011, **84**, 312-319.
40. L. –L. Lv, Y. Cao, D. Liu, M. Xu, H. Liu, R. –N. Tang, K. –L. Ma and B. –C. Liu, *Int. J. Biol. Sci.,* 2013, **9**, 1021-1031.
41. S. Sanjabi, *Anti-Corros. Method Mater.*, 2011, **58,** 245-249.
42. F. Zhang, K. Sautter, A. M. Larsen, D. A. Findley, R. C. Davis, H. Samha and M. R. Linford, *Langmuir*, 2010, **26**, 14648-14654.
43. S. Sun, D. G. Thompson, D. Graham and G. J. Leggett, *J. Mater. Chem.*, 2011, **21**, 14173-14177.
44. A. A. Freitas and J. P. de Magalhães, *Mutation Res.*, 2011, **728**, 12-22.
45. H. Liu and R. M. Crooks, *J. Am. Chem. Soc.*, 2011, **133**, 17564-17566.
46. R. J. Bryant, T. Pawlowski, J. W. F. Catto, G. Marsden, R. L. Vessella, B. Rhees, C. Kuslich, T. Visakorpi and F. C. Hamdy, *Br. J. Cancer*, 2012, **106**, 768-774.
47. R. Burton-Opitz, R. Dinegar, *Am. J. Physiol.*, 1918, **47**, 220-230.

Table 1. DNA oligonucleotide names and sequences (from 5' to 3'); [C3Amino] = primary amine group at the end of a 3 carbon spacer, [AminoC6] = primary amine group at the end of a 6 carbon spacer. Single-base mismatches are shown in blue.

DNA Oligonucleotide Name	Sequence
Model receptor 1	CCAACTATCAA[C3Amino]
Model receptor 2	[AminoC6]CAACTCCATCA
Model target	TTGATAGTTGGTGATGGAGTTG
Total mismatch	CATAACCGATATATTCGGTCGC
6th base-3' end mismatch	TTGATAGTTGGTGATGAAGTTG
6th base-5' end mismatch	TTGATTGTTGGTGATGGAGTTG
2nd base-5' end mismatch	TAGATAGTTGGTGATGGAGTTG
11th base-5' end mismatch	TTGATAGTTGTTGATGGAGTTG
Mir-200c-3p receptor 1	CGGCAGTATTA[C3Amino]
Mir-200c-3p receptor 2	[AminoC6]TCCATCATTACC
Mir-200c-3p	TAATACTGCCGGGTAATGATGGA
Mir-107 receptor 1	ACAATGCTGCT[C3Amino]
Mir-107 receptor 2	[AminoC6]TGATAGCCCTGT
Mir-107	AGCAGCATTGTACAGGGCTATCA

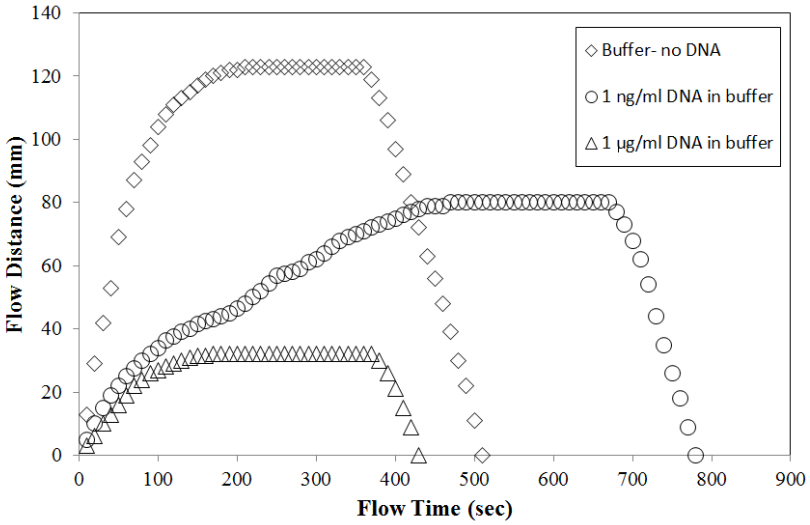

Figure 1. Flow distance as a function of flow time for buffer lacking DNA and two different model target concentrations in microchannels coated with model receptors 1 and 2. The flow distance for buffer increases with flow time until reaching a plateau in ~3 min. 1 ng/mL target takes 8 min to travel ~80 mm where it plateaus, and 1 µg/mL target takes ~3 min to travel ~30 mm where it plateaus.

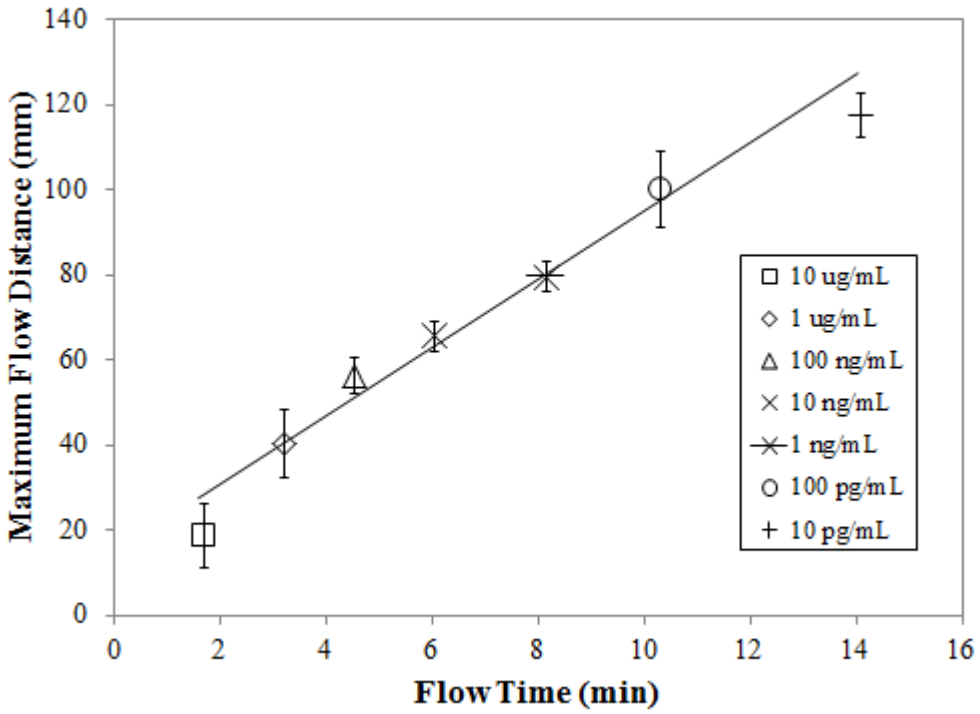

Figure 2. Maximum flow distance as a function of flow time in microchannels coated with model receptors 1 and 2 for different model target concentrations in buffer; best fit equation: $y = 7.79 \pm 0.38\ x + 14.9 \pm 3.1$, $R^2 = 0.956$. Each symbol represents the mean of 3 different measurements, and the error bars indicate ± one standard deviation.

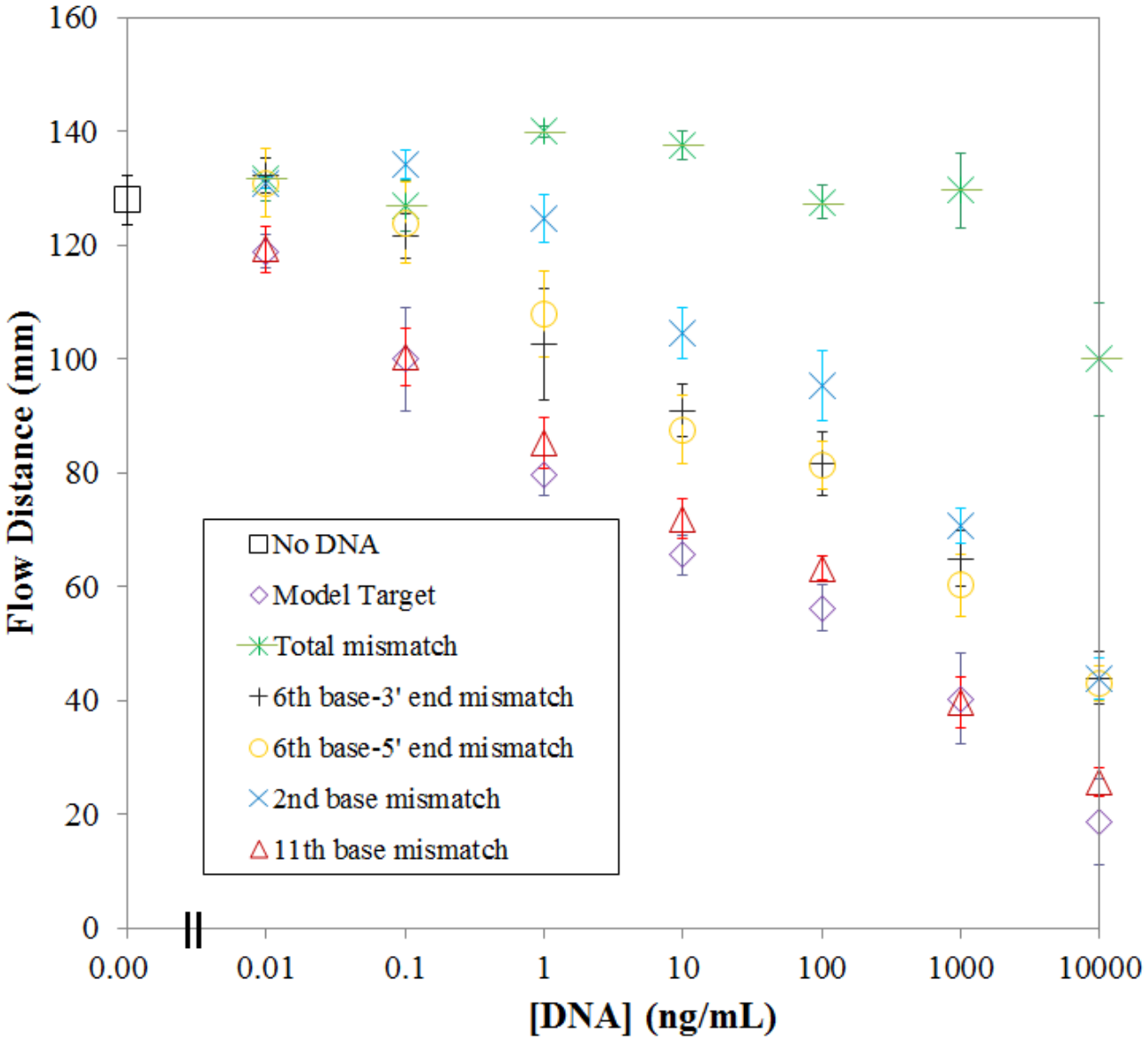

Figure 3. Maximum flow distance as a function of logarithm of DNA concentration for complementary and mismatched sequences in microchannels coated with model receptors 1 and 2. Each symbol represents the mean of 3 different measurements, and the error bars indicate ± one standard deviation.

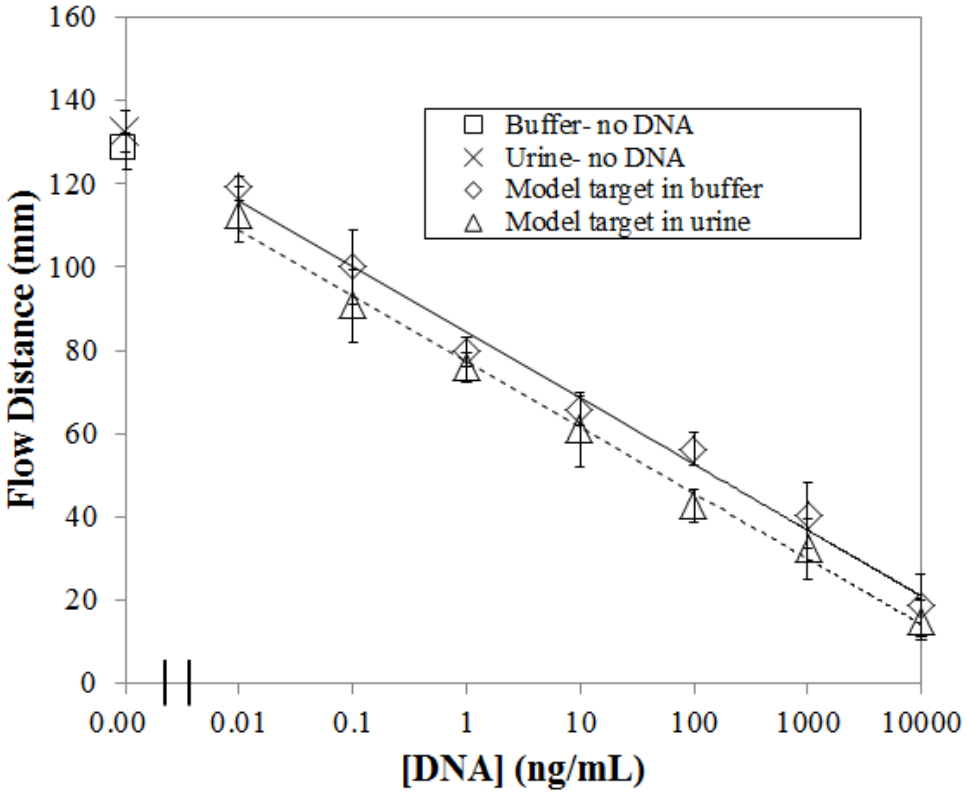

Figure 4. Flow distance as a function of logarithm of model target concentration in buffer (solid line), best fit equation: y = -15.84±0.67 log(x) + 84.4±1.5; and synthetic urine (dashed line), best fit equation: y = -15.78±0.68 log(x) + 77.3±1.5. Each symbol represents the mean of 3 different measurements, and the error bars indicate ± one standard deviation.

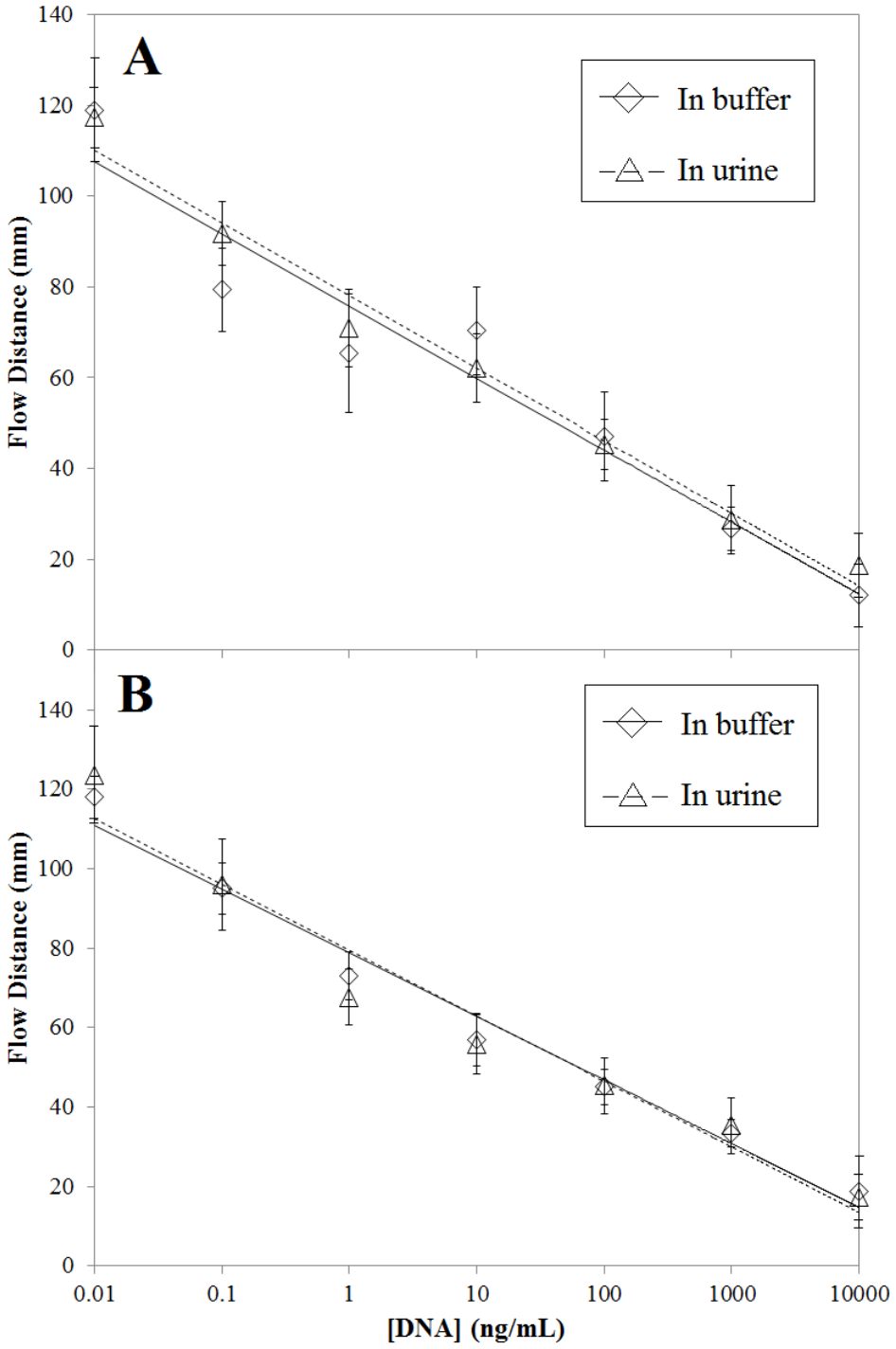

Figure 5. Flow distance in receptor-derivatized microchannels as a function of logarithm of concentration of (A) mir-200c-3p in buffer (solid line), best fit equation: y = -15.9±1.3 log(x) + 75.8±3.0; and synthetic urine (dashed line), best fit equation: y = -15.99±0.84 log(x) + 78.1±1.9, and (B) mir-107 in buffer (solid line), best fit equation: y = -16.05±0.78 log(x) + 78.9±1.7; and synthetic urine (dashed line), best fit equation: y = -16.5±1.1 log(x) + 79.5±2.6. Each symbol represents the mean of 3 different measurements, and the error bars indicate ± one standard deviation.